# Electrocatalytic Hydrogen Evolution in Acidic Water with Molecular Cobalt Tetraazamacrocycles

Charles C. L. McCrory,[†] Christopher Uyeda,[†] and Jonas C. Peters*

Department of Chemistry and Chemical Engineering, California Institute of Technology, 1200 East California Boulevard, Pasadena, California 91125, United States

S *Supporting Information*

ABSTRACT: A series of water-soluble molecular cobalt complexes of tetraazamacrocyclic ligands are reported for the electrocatalytic production of H_2 from pH 2.2 aqueous solutions. The comparative data reported for this family of complexes shed light on their relative efficiencies for hydrogen evolution in water. Rotating disk electrode voltammetry data are presented for each of the complexes discussed, as are data concerning their respective pH-dependent electrocatalytic activity. In particular, two diimine−dioxime complexes were identified as exhibiting catalytic onset at comparatively low overpotentials relative to other reported homogeneous cobalt and nickel electrocatalysts in aqueous solution. These complexes are stable at pH 2.2 and produce hydrogen with high Faradaic efficiency in bulk electrolysis experiments over time intervals ranging from 2 to 24 h.
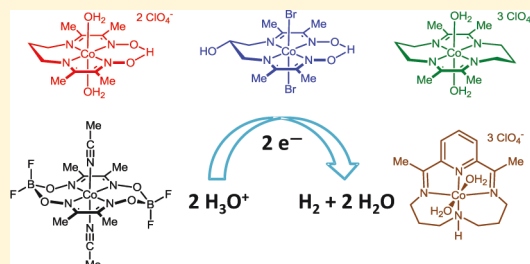
■ INTRODUCTION

The electrocatalytic production of hydrogen from aqueous acids by catalysts composed of earth-abundant elements is a convenient strategy for the storage of intermittent renewable energy.[1] A number of discrete molecular cobalt[2,3] and nickel[4,5] complexes have been shown to electrocatalytically evolve hydrogen in organic solvents with high Faradaic yields and at comparatively low overpotentials. However, relatively few molecular catalysts have been studied for hydrogen evolution in aqueous media,[2d,g,3a−d,h,4,6,7] an important consideration for the application of these catalysts to the design of solar water-splitting devices.[1]

One family of complexes that has been studied as H_2-evolving catalysts in aqueous solutions are cobalt complexes of dimethylglyoxime, $Co(dmgH)_2$, following early work by Chao and Espenson.[7a] However, $Co(dmgH)_2$ suffers from acid instability[8] and operates at rather negative potentials.[2b] Electrocatalytic studies of these catalysts in aqueous solutions at mercury electrodes have moreover been complicated by the strong adsorption of the complex to mercury, which facilitates demetalation and ligand hydrogenation.[9]

The related complex $Co(dmgBF_2)_2$ (**3**) and other cobalt tetraazamacrocycles have shown promise as electrocatalysts with similar activity to $Co(dmgH)_2$ under nonaqueous conditions but at significantly more positive potentials.[2a−h] As an initial step toward studying their electrocatalytic activity in water, we previously reported that glassy carbon electrodes chemically modified with complex **3** catalyze proton reduction from pH 2 solutions with an onset at only 0.24 V negative of the thermodynamic potential.[2g] While encouraging, the specific nature of the resulting catalyst on the surface was not well-
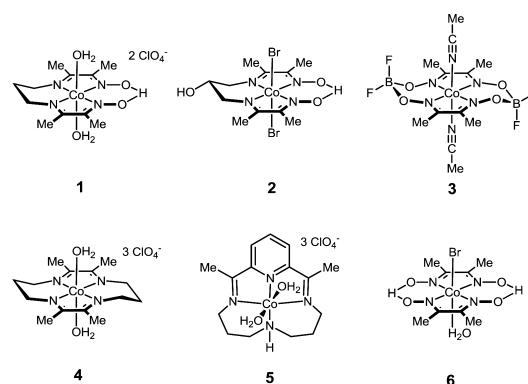
Figure 1. Cobalt complexes of tetraazamacrocycle ligands: Co[(DO)-(DOH)pn(OH₂)₂](ClO₄)₂ (**1**), Co(DO)(DOH)OH-pnBr₂ (**2**), Co-(dmgBF₂)₂(MeCN)₂ (**3**), [Co(TIM)(OH₂)₂](ClO₄)₃ (**4**), [Co(CR)-(OH₂)₂](ClO₄)₃ (**5**), and Co(dmgH)₂(H₂O)Br (**6**).

defined, making detailed mechanistic inferences challenging. Herein, we report that the diimine−dioxime cobalt complexes **1** and **2**, as well as complex **5** (Figure 1), are efficient homogeneous catalysts for hydrogen evolution in acidic aqueous solutions and operate with fast rates and high Faradaic efficiency at unusually low overpotentials by comparison with other molecular electrocatalysts that have been studied in water. The activities of these catalysts are directly compared to the broader family of tetraazamacrocyclic complexes shown in Figure 1.

RESULTS

In order to generate water-soluble complexes, we explored modifications to the carbon backbone of the ancillary ligand to include polar hydroxy functionality (**2**) as well as the incorporation of neutral axial ligands that would render the complexes cationic (**1**, **4**, and **5**). The latter strategy proved to be particularly straightforward, allowing a family of related complexes to be studied as solution-phase species. The identity and purity of all complexes were determined spectroscopically. Additionally, single crystals of **1** suitable for X-ray diffraction were obtained, showing H_2O coordinated to the axial sites (Figure 2).
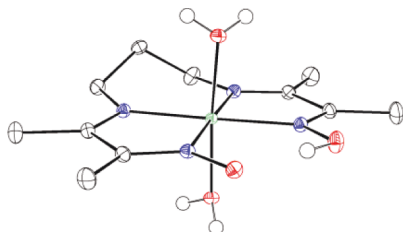

Figure 2. Solid-state structure of **1**. ClO_4^- counterions and hydrogen atoms bound to carbon are omitted for clarity. Thermal ellipsoids are displayed at 50% probability. Hydrogen atoms bound to heteroatoms were located in the difference map.

Cyclic voltammetry experiments were conducted in pH 2.2 aqueous phosphate buffer in order to assess the catalytic activity of **1**−**6**. In all cases, voltammograms collected under Ar or H_2 atmosphere were identical. All complexes exhibited an accessible $Co^{III/II}$ couple at potentials positive of 0 V versus standard calomel electrode (SCE). In cathodic scans of complex **1**, an irreversible reductive peak is observed at −0.76 V that is consistent with a catalytic process at potentials significantly positive of the onset of proton reduction by the electrode (Figure 3). Complex **2** exhibits nearly identical electrochemical behavior as complex **1**. For comparison, the thermodynamic potential for H_2 evolution at pH 2.2 is −0.37 V versus SCE.[10]

Complexes **3** and **5** display initial irreversible reduction peaks of relatively low current density at −0.63 and −0.77 V, respectively, followed by steadily increasing currents at more negative potentials. In the case of complex **3**, the peak at −0.63 V is attributed to a $Co^{II/I}$ couple due to its similar current density to the broad $Co^{III/II}$ feature. For complex **5**, the peak at −0.77 V is likely also related to the $Co^{II/I}$ couple but shows an increased current density compared to the $Co^{III/II}$ couple that is consistent with some catalytic activity at this potential. Complex **4** shows an irreversible reductive feature that appears to be composed of two overlapping irreversible reductions at −0.74 and −0.82 V. Cyclic voltammograms of solutions containing complex **6** or $Co(ClO_4)_2 \cdot 6H_2O$ were nearly identical to background scans with the glassy carbon electrode in the absence of catalyst.

To directly compare the potential-dependent catalytic activity of complexes **1**−**5**, we determined the rate of electron delivery to the catalyst normalized for catalyst delivery to the surface, n_{app}, at a rotating disk electrode at 400 rpm.[2i] n_{app} is the apparent number of electrons delivered to a catalyst molecule in the electrocatalytic process before the catalyst molecule is transported away from the electrode, and it is related to the electrocatalytic current density normalized for the delivery of
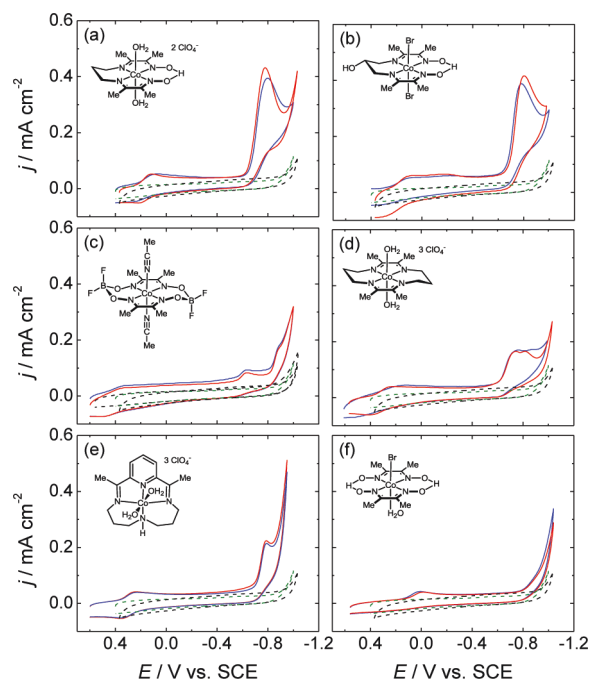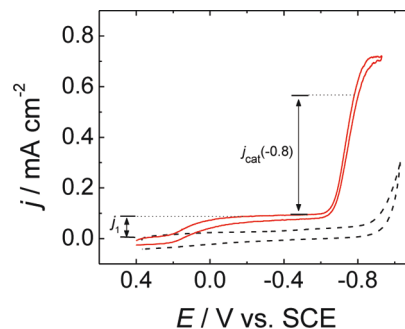

Figure 3. Cyclic voltammograms in 0.1 M phosphate buffer at pH 2.2 in the absence (black dashed line) and presence of 0.3 mM catalyst **1** (a), **2** (b), **3** (c), **4** (d), **5** (e), or **6** (f) under H_2 (red solid line) or Ar (blue solid line). The green dashed line is the cyclic voltammogram of 0.3 mM $Co(ClO_4)_2 \cdot 6H_2O$ under the same conditions with no other catalyst present. Conditions: 0.1 M $NaClO_4$ supporting electrolyte, 0.195 cm^2 glassy carbon working electrode, scan rate = 0.05 V/s.

the catalyst to the surface as defined by[11]

$$n_{app} = \frac{j_{cat}}{j_1} \tag{1}$$

For the catalysts investigated here, j_1 is the plateau current density for the $Co^{III/II}$ couple and j_{cat} is the catalytic current density as shown in the representative steady-state voltammogram in Figure 4 for catalyst **1** in 0.1 M phosphate buffer at pH 2.2 (for complexes **2**−**5**, see Figures S1−S4 in Supporting Information).

The potential dependent n_{app} for each catalyst is shown in Figure 5. Complex **3** shows $n_{app} \approx 1$ at potentials between

Figure 4. Rotating disk electrode voltammogram at 400 rpm in 0.1 M phosphate buffer at pH 2.2 in the absence (black dashed line) and presence (red solid line) of 0.3 mM complex **1**. j_1 is the plateau current density for the $Co^{III/II}$ reduction. $j_{cat}(E)$ is the catalytic current density and is measured from j_1. $j_{cat}(-0.8) = 0.51$ mA·cm^{-2} as shown in the figure. Conditions: 0.1 M $NaClO_4$ supporting electrolyte, scan rate = 0.025 V/s, H_2 atmosphere.
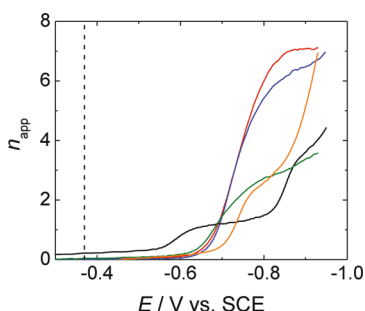
Figure 5. Rate of electron delivery, n_{app}, in the electrocatalytic hydrogen evolution from buffered pH 2.2 aqueous solution by **1** (red line), **2** (blue line), **3** (black line), **4** (green line), and **5** (orange line). The vertical dashed line is −0.37 V, the thermodynamic potential of the reduction of 2 H+ to H_2 under 1 atm H_2 at pH 2.2.[10]

ca. −0.6 and −0.8 V, presumably from the reduction of Co^{II} to Co^{I} prior to electrocatalytic H_2 evolution. For catalysts **3** and **5**, modest catalysis is observed at potentials positive of ca. −0.85 V, at which point a rapidly increasing n_{app} is observed that remains potential-dependent throughout the range investigated. Complexes **1** and **4** show the same electrocatalytic onset at −0.63 V; however, **1** operates with significantly higher n_{app} at any given potential. Complexes **1** and **2** exhibit nearly identical electrocatalytic activity at every potential.

In order to assess the Faradaic efficiency for H_2 evolution, controlled-potential electrolyses at −0.93 V were conducted in stirred 0.l M phosphate buffer solutions, pH 2.2, containing the catalyst at 0.3 mM concentration. The yield of H_2 was determined by sampling the headspace of the sealed electrolysis cell after a 2-h period and analyzing the mixture by gas chromatography. Representative plots of the charge passed over time during the controlled-potential electrolyses for each complex are shown in Figure S5 (Supporting Information), and the pertinent results are summarized in Table 1.

Table 1. Charge Passed during 2-h Bulk Electrolyses and Corresponding Faradaic Efficiencies.[a]

catalyst	q^b/C	f^c/%	TON^d
none	4.2	97	
1	50.3	81	23
2	38.2	80	18
3	35.0	79	16
4	12.0	30	2
5	32.7	92	17

[a]All bulk electrolyses were run in duplicate, at −0.93 V versus SCE, and the average values are reported. [b]Charge delivered during a controlled-potential electrolysis. [c]Faradaic efficiency determined by GC analysis. [d]Turnover number from the equivalents of hydrogen produced per catalyst equivalent over the electrolysis period.

Complex **1** passes the most charge during 2-h controlled-potential electrolyses and operates with a ca. 80% Faradaic efficiency, corresponding overall to 23 turnovers of the catalyst. Complex **2** performs with nearly Faradaic identical efficiency but at slightly attenuated rates. An order of magnitude less charge was passed in electrolyses conducted with no catalyst present. During the course of the electrolysis experiment, an irreversible color change from pale yellow to colorless was observed in the solution of catalyst **1** (see Figure S6 in Supporting Information). In the absence of an applied potential

under otherwise identical conditions, this color change was not observed over 2 h (Figure S7, Supporting Information) or 24 h (Figure S6, Supporting Information). To test whether catalytically active species are deposited onto the electrode surface, subsequent to the electrolysis, the electrode was rinsed with water and electrolysis at −0.93 V was run for an additional 2 h in a 0.1 M phosphate buffer at pH 2.2 with no catalyst present in solution. During this period, ca. 3.4 C of charge was passed, a similar magnitude as is observed for electrolyses conducted with freshly polished electrodes (Figure 6).
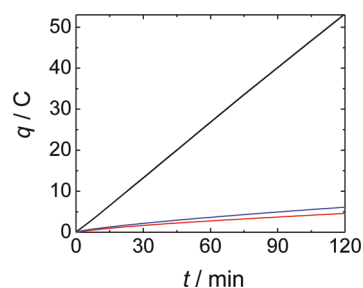

Figure 6. Controlled potential electrolysis in aqueous solution at pH 2.2 of **1** (black line) showing cumulative charge over time with an applied potential of −0.93 V vs SCE. After a 2-h electrolysis experiment, the electrode was rinsed with water, and the controlled-potential electrolysis was repeated in a fresh pH 2.2 solution with no catalyst present (blue line). The electrolysis of a bare glassy carbon electrode in a catalyst-free solution is shown for comparison (red line). Conditions: 0.1 M $NaClO_4$ supporting electrolyte.

Complex **3** evolves H_2 at slower rates than **1** but with a similar 79% Faradaic efficiency. Complex **5** exhibits the highest Faradaic efficiency for hydrogen production, although at significantly slower rates than **1**. During the electrolysis, the initially yellow solution of complex **5** turns red, but returns to yellow upon exposure to air. This is consistent with reduction of the Co(III) precatalyst to the Co(II) oxidation state under electrolysis conditions.[2c,i] Of the complexes evaluated, **4** exhibits both the slowest rates as well as the lowest yields of H_2. Additionally, the current was observed to decrease over the 2-h electrolysis period, suggesting that catalyst **4** decomposes to an inactive species under these conditions.

In order to determine whether complex **1** retains activity over longer time periods, a 24-h controlled-potential electrolysis at −0.93 V was conducted in stirred 0.1 M phosphate buffer solutions, pH 2.2, containing the catalyst at 0.3 mM concentration. A total of 295 C was passed during the electrolysis and 32 mL of gaseous product were evolved, as determined volumetrically. This corresponds to a Faradaic yield of 86% with an estimated error of ±10%. Gas chromatography was used to confirm the presence of H_2 in the displaced headspace gas. The rate of H_2 evolution determined from the 24-h bulk electrolysis experiment is ca. 68.4 L of H_2·(mol of catalyst)$^{-1}$·h^{-1}.

To explore the pH dependence of electrocatalytic activity for the four catalysts that showed the highest Faradaic efficiencies, complexes **1**−**3** and **5**, cyclic voltammetry experiments were conducted in 0.1 M solutions of $HClO_4$ with a measured pH = 1.2, phosphate buffer at pH = 2.2, acetate buffer at pH = 4.8, and phosphate buffer at pH = 7.0 (Figure 7). For catalysts **1** and **2**, the peak potential of the first reduction subsequent to the $Co^{III/II}$ couple, E_p, was observed to shift to more negative potentials with increasing pH at a rate of ca. −0.06 V per pH
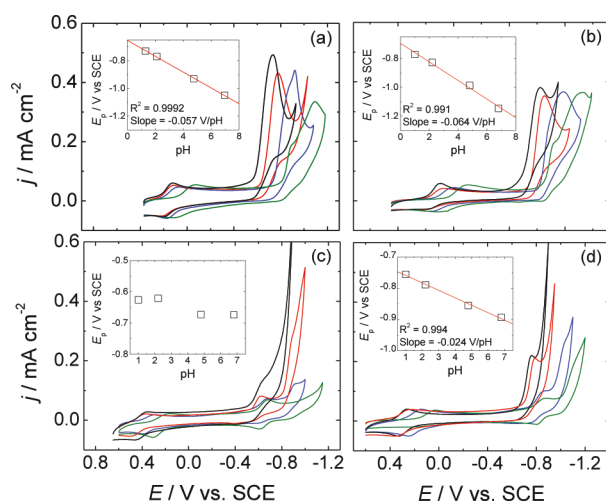
Figure 7. Cyclic voltammograms of 0.3 mM **1** (a), **2** (b), **3** (c), and **5** (d) in aqueous solutions at pH = 1.2 (black lines), pH = 2.2 (red lines), pH = 4.8 (blue lines), and pH = 7.0 (green lines). (Insets) Plots of peak potential of the first reductive wave subsequent to the Co$^{III/II}$ couple as a function of pH. Conditions: supporting electrolyte 0.1 M NaClO$_4$, scan rate = 0.05 V/s, H$_2$ atmosphere.

unit (Figure 7a,b, insets). For these complexes, there is no significant decrease in the electrocatalytic peak current density j_p as a function of increasing pH.

For catalyst **3**, there is no clear trend in E_p as a function of pH (Figure 7c, inset), but there is a marked increase in the magnitude and onset potential of the subsequent catalytic wave. At pH 7, a reversible wave is seen with $E^0 = -0.64$ V. This lends further support for the assignment of this first reductive wave subsequent to the Co$^{III/II}$ couple as the Co$^{II/I}$ couple. At all other pHs, the reduction event at this potential is irreversible, and a subsequent catalytic process is observed at more negative potentials. In the case of catalyst **5**, there is a shift in E_p of -0.024 V per pH unit (Figure 7d).

◼ DISCUSSION

The parent, proton-bridged Co(dmgH)$_2$ complex (**6**) exhibited no electrocatalytic reduction under aqueous conditions within the window of the glassy carbon electrode. Incorporation of BF$_2$ bridges within the macrocycle, however, results in an anodic shift in the reduction potential. Thus, Co(dmgBF$_2$)$_2$ (**3**) evolves H$_2$ from pH 2.2 water with a Faradaic efficiency of nearly 80%. Slow H$_2$ production by complex **3** has been previously reported with CrCl$_2$ as a chemical reductant in 0.25 M HCl;[12] however, it has been observed that turnover-dependent degradation occurs in pH 2.5 citrate buffers using titanium(III) citrate as a chemical reductant.[13] This latter result is qualitatively consistent with our findings.

Of the complexes that were evaluated, catalyst **1** exhibited the highest rates of H$_2$ evolution at the most positive potentials. Over a 2-h period, catalytic activity remained constant, and hydrogen was produced in 81% yield. The cumulative charge passed during this period, corrected for the Faradaic efficiency, corresponds to a catalyst turnover number (TON) of 23. This value is similar in magnitude to those reported for related tetraazamacrocycle complexes[2e,i] and a Ni(diphosphine)$_2$ complex[14] in acetonitrile using organic acids and a carbon working electrode. The TON, while useful for the comparison of catalytic activity measured under comparable experimental conditions, is highly limited by mass transport to the electrode

and is therefore not an indication of the intrinsic rate at which the elementary chemical steps proceed.

An additional method that has been used to estimate catalytic rates is based on an approximate model for pseudo-first-order catalytic systems:[11c,14,15]

$$\frac{j_c}{j_p} = \frac{2}{0.446} \sqrt{\frac{RTk_{obs}}{F\upsilon}} \qquad (2)$$

Here j_c is the catalytic plateau current density, j_p is the noncatalytic peak current (here taken from the reversible reduction peak associated with the Co$^{III/II}$ redox couple), R is the ideal gas constant, $T = 298.15$ K, F is Faraday's constant, and υ is the scan rate. Although this approach has only rigorously been verified for simple EC′ mechanisms under pseudo-first-order conditions,[11c,15] it has nevertheless been applied to estimate catalytic rates of systems with more complicated or undetermined catalytic mechanisms.[2c,3i,5c,d,6a]

For catalyst **1**, j_{cat} is roughly constant at fast scan rates, $\upsilon \geq$ 6 V/s (Figure S9, Supporting Information), and a plot of j_c/j_p as a function of $\upsilon^{-1/2}$ is linear (Figure S10, Supporting Information). $k_{obs} = 295$ s^{-1} was determined from the slope of the plot. This rate is similar to that reported recently for a related cobalt macrocycle in pH 4 solution but at a potential that is ca. 0.5 V more positive.[6a] An important caveat is that the shape of the CV for **1** under catalytic conditions does not reach a plateau even at scan rates up to 10 V/s. Furthermore, there is no apparent dependence of the peak current on pH (Figure 7a). Both of these observations suggest that the catalyst does not operate by a simple EC′ mechanism. Thus, the k_{obs} determined from this method is provided for comparison with related H$_2$-evolving catalysts in the literature where the authors have employed the Savéant relationship expressed in eq 2 to estimate rate.

There are several factors that may contribute to Faradaic efficiency less than unity for complex **1** and the observation of a color change in the electrolysis solution over time. In putative Co$^{II/I}$ catalytic cycles, one reducing equivalent per molecule of the Co^{III} precatalyst is needed in order to enter the cycle. Additionally, it is possible that the unsaturated bonds of the ligand are susceptible to reduction, resulting in the formation of a new solution species that retains catalytic activity. The possibility of reductive deposition of an electrocatalytically active surface-bound species can be excluded, given the inactivity of a freshly rinsed electrode subsequent to a 2-h bulk electrolysis. Over extended 24-h bulk electrolyses, the average current was observed to decrease relative to the initial 2-h period; however, Faradaic efficiency for H$_2$ production was maintained. At various time points, yields between 80% and 100% were measured with a final cumulative yield of 86% (Table S1, Supporting Information).

The catalytic peak potential of complexes **1** and **2** exhibited a Nernstian response of ca. -60 mV per pH unit, consistent with a one-proton and one-electron process. This is consistent with the initial reduction of Co^{II} to Co^I being facilitated by the coordination of a proton to the complex. A qualitatively similar dependence of E_p on acid strength has been observed for Co(DO)(DOH)pnBr$_2$ under nonaqueous conditions. It has been proposed by Artero and co-workers[2e] that this dependence can be attributed to protonation of the ligand oxime groups. It is noteworthy in this context that neither the BF$_2$-bridged analogue studied in acetonitrile nor the recently reported Co(PY5) complexes[3h] studied in water exhibit this dependence of the catalytic wave on acidity.

The BF$_2$-bridged complex **3** shows no shift in E_p as a function of pH, but there is a negative shift in the onset potential of the catalytic wave. This suggests that there is no protonation event coupled to the reduction of Co^{II} to Co^{I} in complex **3**, and instead the pH dependence of the subsequent electrocatalytic wave might be due to a proton-coupled electron transfer step. It is worth noting that there is an increase in the catalytic current for complex **3** with acid that is not evident in complexes **1** and **2**, again suggesting that in the case of catalysts **1** and **2** the proton is associated in a pre-equilibrium step prior to electrocatalytic proton reduction.

For complex **5**, there is a more complicated pH dependence for E_p of −0.24 V per pH unit. This is close to a −30 mV per pH unit dependence consistent with the Nernstian response for a two-electron and one-proton reduction and is qualitatively similar to the −0.26 V per pH unit dependence reported for the noncatalytic Co$^{II/I}$ couple of Co(PY5).[3h] There is also a ca. −60 mV per pH unit dependence on the Co$^{III/II}$ couple for complex **5** between pH 2.2 and 7 (Figure S8, Supporting Information). This is consistent with an equilibrium protonation of the ligand, presumably at the coordinated amine. An electrocatalytic mechanism that is consistent with both pH dependences might involve an initial one-electron, one-proton reduction to form a protonated Co^{II} complex, followed by a subsequent catalytic reduction by two electrons and one proton to generate H$_2$.

The electrocatalytic H$_2$-evolving activity of complexes **1** and **2** compare favorably to other reported homogeneous cobalt and nickel catalysts, many of which operate at significantly higher overpotentials[3c] or with lower Faradaic efficiencies.[3b] Cobalt complexes with nitrogen donor ligands have recently emerged as a particularly promising class of catalysts, evolving H$_2$ in neutral water at fast rates. In particular, a series of cobalt pentapyridine complexes[3h] and a cobalt bis(iminopyridine) complex[6a] were shown to be active toward hydrogen evolution under neutral aqueous conditions. In both cases, a pH-independent electrocatalytic onset was observed at −1.2 to −1.4 V versus SCE at a mercury electrode. The cobalt diimine−dioxime complexes **1** and **2** by contrast exhibit significantly more positive onset potentials and operate with high Faradaic efficiency under acidic conditions. Two complexes reported by Grätzel and co-workers,[3b] Co(sep)$^{3+}$ and Co(C$_5$H$_4$CO$_2$H)$_2$)$_2$$^+$, are also noteworthy, showing low-overpotential H$_2$ evolution in water at a mercury pool electrode but with much lower Faradaic efficiencies (55% and 42%, respectively).

Evaluation of electrocatalytic H$_2$ evolution rates between the complexes described here and a broader range of homogeneous catalysts reported in the literature are complicated by differences in experimental setup. Specifically, both the area of the working electrode and the rate of catalyst delivery to the electrode must be well-defined for meaningful comparison.[16] Moreover, the use of different working electrodes (i.e., graphite, glassy carbon, Hg, etc.) can lead to very different electrochemical responses, based on the extent to which they facilitate catalyst adsorption.[6b,9,17] Further studies of electrocatalytic H$_2$ production under identical conditions by rotating disk voltammetry are warranted to accurately compare the relative potential-dependent electron-delivery rates of **1** and other molecular H$_2$-evolving complexes.

CONCLUSION

A series of readily accessible, water-soluble cobalt tetraazamacrocyclic complexes are shown to evolve H$_2$ from water at pH 2.2. In particular, complexes **1** and **2** show similar activity for H$_2$ production with a Faradaic efficiency of ca. 80% in 2-h controlled-potential electrolysis experiments at −0.93 V with a putative catalytic onset at −0.63 V, which is only 0.26 V negative of the thermodynamic potential. Complex **1** was shown to continue to evolve H$_2$ over a 24-h period. In addition, complex **5** was shown to operate at the same overpotential with high Faradaic efficiency, albeit with a more negative catalytic onset. In a comparison of the potential-dependent rates for other related cobalt complexes, complexes **1** and **2** show the fastest n_{app} at potentials positive of −0.93 V. These complexes complement other high-efficiency homogeneous cobalt and nickel electrocatalysts reported in the literature that operate near neutral pH but require significantly higher overpotentials for H$_2$ evolution.[3h,6a]

EXPERIMENTAL SECTION

Materials. All electrolyte solutions were prepared with water deionized with the Thermo Scientific Barnsted Nanopure water purification system (18.2 MΩ·cm resistivity). Phosphoric acid (H$_3$PO$_4$), monobasic sodium phosphate (NaH$_2$PO$_4$), dibasic sodium phosphate (Na$_2$H$_2$PO$_4$), and sodium perchlorate monohydrate (NaClO$_4$) were ACS-grade and used as received (Sigma−Aldrich). HClO$_4$(aq) (67−72%) was Trace-Select grade and used as received (Fluka). All other gases and chemical reagents were purchased from commercial vendors and used as received. The pH of buffer solutions were measured with a benchtop VWR Symphony pH meter with an Accumet Symphony Posi-PHIo Ag/AgCl electrode.

Synthesis of Cobalt Complexes. All manipulations of cobalt(III) complexes were performed under ambient atmosphere without protection from water or oxygen. Co-(dmgH$_2$)$_2$Br(H$_2$O)[18] and Co(dmgBF$_2$)$_2$(MeCN)$_2$ (**3**)[19] were prepared according to the previously reported procedure.

[Co(DO)(DOH)pn(OH$_2$)$_2$](ClO$_4$)$_2$ (1) was prepared according to the general procedure of Costa et al.[20] Co(DO)(DOH)pnBr$_2$ (458.0 mg, 1.0 mmol, 1.0 equiv) was suspended in 10 mL of H$_2$O. AgNO$_3$ (322.8 mg, 1.9 mmol, 1.9 equiv) was added as a solid. After stirring in the dark for 2 h, the reaction mixture was filtered through a Celite pad and washed with three portions of H$_2$O. The filtrate was concentrated to a total volume of 10 mL, and 5 mL of concentrated perchloric acid was added. The solution was allowed to stand at room temperature for 24 h, during which time a crystalline solid precipitated. The precipitate was isolated by filtration through a fritted glass funnel, washed with several portions of Et$_2$O, and dried under vacuum to yield 309.9 mg of [Co(DO)(DOH)pn(OH$_2$)$_2$](ClO$_4$)$_2$ (0.58 mmol, 58% yield). Single crystals suitable for X-ray diffraction were obtained in this manner. ^{1}H NMR (400 MHz, D$_2$O) δ = 4.31−4.11 (m, 4H), 2.83 (s, 6H), 2.71 (s, 6H), 2.47−2.29 (m, 2H). UV−vis (H$_2$O) λ_{max}, nm (ε) 301 (3500 M^{-1}·cm^{-1}), 219 (20 000 M^{-1}·cm^{-1}). Anal. Calcd for C$_{11}$H$_{23}$Cl$_2$CoN$_4$O$_{12}$: C, 24.78; H, 4.35; N, 10.51. Found: C, 24.82; H, 4.26; N, 10.44. ESI-MS m/z (relative intensity): [M − 2(H$_2$O) + H]$^+$ 299.0 (100%), [M − H$_2$O − H]$^+$ 314.8 (50%).

Co(DO)(DOH)pnOHBr$_2$ (2) was prepared according to the general procedure described by Costa et al.[21] from 1,3-diamino-2-propanol. ^{1}H NMR (300 MHz, CD$_3$CN) δ = 19.33 (s, 1 H), 4.75−4.56 (m, 1H), 4.17 (br m, 4H), 3.90 (d, J = 10.0 Hz, 1H), 2.63 (s, 6H), 2.55 (s, 6H). UV−vis (MeCN) λ_{max}, nm (ε) 591 (68 M^{-1}·cm^{-1}), 370 (sh, 2300 M^{-1}·cm^{-1}), 298 (17 000 M^{-1}·cm^{-1}), 232 (13 000 M^{-1}·cm^{-1}). ESI-MS m/z (relative

3168

dx.doi.org/10.1021/ja210661k | *J. Am. Chem. Soc.* 2012, 134, 3164−3170

intensity): $[M - 2Br]^+$ 314.1 (90%), $[M - Br + OH]^+$ 409.9 (100%), $[M - Br + MeCN]^+$ 433.8 (85%).

$[Co(TIM)(OH_2)_2](ClO_4)_3$ (**4**) was prepared according to the general procedure described for complex **1**, starting from $[Co(TIM)Br_2]Br.^{22}$ ^{1}H NMR (400 MHz, D_2O) δ = 4.16−4.04 (m, 8H), 2.82 (s, 12H), 2.39−2.27 (m, 4H). UV−vis (H_2O) λ_{max}, nm (ε) 514 (60 $M^{-1}\cdot cm^{-1}$), 352 (980 $M^{-1}\cdot cm^{-1}$). ESI-MS m/z (relative intensity): $[M - 2H]^+$ 341.0 (65%), $[M - 2(H_2O)]^+$ 307.3 (25%), $[M - H_2O - H + ClO_4]^+$ 423.0 (85%), $[M - H_2O - H]^{2+}$ 162.0 (100%).

$[Co(CR)(OH_2)_2](ClO_4)_3$ (**5**) was prepared according to the general procedure described for complex **1**, starting from $[Co(CR)Br_2]Br.^{23}$ ^{1}H NMR (400 MHz, D_2O) δ = 8.83 (t, J = 8.1 Hz, 1H), 8.69 (d, J = 8.4 Hz, 2H), 4.18 (br d, J = 16.5 Hz, 2H), 3.77 (br t, J = 15.0 Hz, 2H), 3.18−3.00 (m, 4H), 3.03 (s, 6H), 2.57 (br d, J = 15.8 Hz, 2H), 2.17 (br q, J = 13.6 Hz, 2H). UV−vis (H_2O) λ_{max}, nm (ε) 456 (212 $M^{-1}\cdot cm^{-1}$), 275 (sh, 3600 $M^{-1}\cdot cm^{-1}$), 215 (25 000 $M^{-1}\cdot cm^{-1}$). ESI-MS m/z (relative intensity): $[M - 2(H_2O) - 2H]^+$ 315.3 (100%), $[M - 2(H_2O) - H]^{2+}$ 158.1 (60%).

X-ray Crystallography Procedures. X-ray diffraction studies were carried out at the Beckman Institute Crystallography Facility on a Brüker Kappa Apex II diffractometer and solved using SHELX v. 6.14. The crystals were mounted on a glass fiber with Paratone-N oil. Data were collected at 100 K with Mo Kα (λ = 0.710 73 Å) radiation, solved by use of SHELXS, and refined against $F2$ on all data by full-matrix least-squares with SHELXL.[24] X-ray quality crystals were grown as described under Synthesis of Cobalt Complexes.

Other Spectroscopic Measurements. A Varian Mercury 300 MHz spectrometer and a Varian MR 400 MHz spectrometer were used to collect ^{1}H NMR spectra at room temperature. ^{1}H NMR spectra were referenced to the residual solvent peak (D_2O = 4.79, CD_3CN 1.94). UV−vis measurements were taken on a Cary 50 UV/vis spectrophotometer by use of quartz cuvettes with a Teflon screw cap.

Electrochemical Measurements. Electrochemical measurements were recorded with a CH Instruments 630-C electrochemistry analyzer using a CHI version 8.09 software package. Unless otherwise noted, cyclic voltammetry and rotating-disk electrode voltammetry measurements were conducted in 50 mL aqueous solutions of 0.1 M $NaClO_4$ with 0.1 M phosphate buffer at pH 2.2. Unless otherwise noted, all solutions were deaerated with H_2 gas prior to electrochemical analysis, and the solution was blanketed with H_2 during experiments. For each measurement, a 0.195 cm^2 glassy carbon disk electrode was used as the working electrode (Pine Instrument Co.), a Pt wire was used as the auxiliary electrode, and an aqueous Ag/AgCl/saturated KCl electrode was used as the reference electrode (Bioanalytical Systems, Inc.). Ferrocene monocarboxylic acid in an aqueous pH 7 solution with 0.1 M phosphate buffer and 0.1 M $NaClO_4$ was used as an external standard for the reference electrode (E^0 = 0.28 V vs SCE),[25] and all potentials are reported versus SCE. A Pine Instrument Co. MSR-2 rotator was used for rotating-disk electrode voltammetry measurements.

Controlled-potential electrolysis measurements were conducted in a sealed two-chambered H cell where the first chamber held the working and reference electrodes in 65 mL of 0.1 M $NaClO_4$(aq) with 0.3 mM catalyst, and the second chamber held the auxiliary electrode in 25 mL of 0.1 M $NaClO_4$(aq). The two chambers were separated by a fine-porosity glass frit. Glassy carbon plates (12 cm × 3 cm × 1 cm;

Tokai Carbon USA) were used as the working and auxiliary electrodes and submerged such that ca. 64 cm^2 of the plate was in the electrolyte solution. The reference electrode was a Ag/AgCl/saturated NaCl(aq) electrode separated from the solution by a Vycor frit. The cell was purged with N_2 for ca. 20 min and then sealed under an atmosphere of N_2 before the beginning of each electrolysis experiment. For 2-h experiments, the amount of H_2 evolved was quantified from an analysis of the headspace of the first chamber with an Agilent 7890A gas chromotograph (HP-PLOT U, 30 m, 0.32 mm i.d.; 30 °C isothermal; 1 mL/min flow rate; N_2 carrier gas) using a thermal conductivity detector. The total amount of H_2 produced was determined as the sum of H_2 in the headspace plus dissolved H_2 in the solution calculated by Henry's law, with a constant of 7.8 × 10^{-4} mol·kg^{-1}·atm^{-1}.[26] Faradaic efficiencies were determined by dividing the measured H_2 produced by the amount of H_2 expected on the basis of charge passed during the controlled-potential electrolysis measurements.

For longer 24-h experiments, the amount of H_2 evolved was quantified by measuring the volumetric displacement of headspace gas. It is important to note that, for the longer controlled potential electrolysis measurements, it is difficult to maintain equal pressure on both chambers of the H-cell. This can lead to large variances in the determined Faradaic efficiencies between experimental runs and even at different times in the same experiment (see Table S1, Supporting Information). We estimate the error in the reported Faradaic effiencies for 24-h bulk electrolyses to be at least ±10%.

■ ASSOCIATED CONTENT

S Supporting Information

Ten figures and one table as described in the text (PDF) and X-ray structure information (CIF). This material is available free of charge via the Internet at http://pubs.acs.org.

■ AUTHOR INFORMATION

Corresponding Author
jpeters@caltech.edu.

Author Contributions
[†]These authors contributed equally.

Notes
The authors declare no competing financial interest.

■ ACKNOWLEDGMENTS

■ REFERENCES

(1) (a) Grätzel, M. *Acc. Chem. Res.* **1981**, *14*, 376−384. (b) Koelle, U. *New J. Chem.* **1992**, *16*, 157−169. (c) Bard, A. J.; Fox, M. A. *Acc. Chem. Res.* **1995**, *28*, 141−145. (d) Turner, J. A. *Science* **2004**, *305*, 972−974. (e) Artero, V.; Fontecave, M. *Coord. Chem. Rev.* **2005**, *249*, 1518−1535. (f) Lewis, N. S.; Nocera, D. G. *Proc. Natl. Acad. Sci. U.S.A.* **2006**, *103*, 15729−15735. (g) Lewis, N. S. *Science* **2007**, *315*, 798−801. (h) Crabtree, G. W.; Dresselhaus, M. S. *MRS Bull.* **2008**, *33*, 421−428.
(2) (a) Hu, X.; Cossairt, B. M.; Brunschwig, B. S.; Lewis, N. S.; Peters, J. C. *Chem. Commun.* **2005**, 4723−4725. (b) Baffert, C.; Artero, V.; Fontecave, M. *Inorg. Chem.* **2007**, *46*, 1817−1824. (c) Hu, X.; Brunschwig, B. S.; Peters, J. C. *J. Am. Chem. Soc.* **2007**, *129*, 8988−8998. (d) Pantani, O.; Anxolabéhère-Mallart, E.; Aukauloo, A.; Millet, P. *Electrochem. Commun.* **2007**, *9*, 54−58. (e) Jacques, P.-A.; Artero, V.; Pecaut, J.; Fontecave, M. *Proc. Natl. Acad. Sci. U.S.A.* **2009**, *106*, 20627−20632. (f) Dempsey, J. L.; Brunschwig, B. S.; Winkler, J. R.;

Gray, H. B. *Acc. Chem. Res.* **2009**, *42*, 1995−2004. (g) Berben, L. A.; Peters, J. C. *Chem. Commun.* **2010**, 398−400. (h) Fourmond, V.; Jacques, P.-A.; Fontecave, M.; Artero, V. *Inorg. Chem.* **2010**, *49*, 10338−10347. (i) McCrory, C. C. L.; Szymczak, N. K.; Peters, J. C. Unpublished results.

(3) (a) Fisher, B. J.; Eisenberg, R. *J. Am. Chem. Soc.* **1980**, *102*, 7361−7363. (b) Houlding, V.; Geiger, T.; Kolle, U.; Grätzel, M. *J. Chem. Soc., Chem. Commun.* **1982**, 681−683. (c) Koelle, U.; Paul, S. *Inorg. Chem.* **1986**, *25*, 2689−2694. (d) Koelle, U.; Infelta, P. P.; Grätzel, M. *Inorg. Chem.* **1988**, *27*, 879−883. (e) Pantani, O.; Naskar, S.; Guillot, R.; Millet, P.; Anxolabéhère-Mallart, E.; Aukauloo, A. *Angew. Chem., Int. Ed.* **2008**, *47*, 9948−9950. (f) Jacobsen, G. M.; Yang, J. Y.; Twamley, B.; Wilson, A. D.; Bullock, R. M.; DuBois, M. R.; Dubois, D. L. *Energy Environ. Sci.* **2008**, *1*, 167−174. (g) Losse, S.; Vos, J. G.; Rau, S. *Coord. Chem. Rev.* **2010**, *254*, 2492−2504. (h) Sun, Y.; Bigi, J. P.; Piro, N. A.; Tang, M. L.; Long, J. R.; Chang, C. J. *J. Am. Chem. Soc.* **2011**, *133*, 9212−9215. (i) Bigi, J. P.; Hanna, T. E.; Harman, W. H.; Chang, A.; Chang, C. J. *Chem. Commun.* **2010**, *46*, 958−960.

(4) Efros, L. L.; Thorp, H. H.; Brudvig, G. W.; Crabtree, R. H. *Inorg. Chem.* **1992**, *31*, 1722−1724.

(5) (a) Wilson, A. D.; Newell, R. H.; McNevin, M. J.; Muckerman, J. T.; Rakowski DuBois, M.; DuBois, D. L. *J. Am. Chem. Soc.* **2005**, *128*, 358−366. (b) Dubois, M. R.; Dubois, D. L. *Acc. Chem. Res.* **2009**, *42*, 1974−1982. (c) Kilgore, U. J.; Roberts, J. A. S.; Pool, D. H.; Appel, A. M.; Stewart, M. P.; DuBois, M. R.; Dougherty, W. G.; Kassel, W. S.; Bullock, R. M.; DuBois, D. L. *J. Am. Chem. Soc.* **2011**, *133*, 5861−5872. (d) Appel, A. M.; Pool, D. H.; O'Hagan, M.; Shaw, W. J.; Yang, J. Y.; Rakowski DuBois, M.; DuBois, D. L.; Bullock, R. M. *ACS Catal.* **2011**, *1*, 777−785.

(6) (a) Stubbert, B. D.; Peters, J. C.; Gray, H. B. *J. Am. Chem. Soc.* **2011**, *133*, 18070−18073. (b) Kellett, R. M.; Spiro, T. G. *Inorg. Chem.* **1985**, *24*, 2373−2377. (c) Abdel Hamid, R.; Abdelhamid, R.; Abdel, H. *Polyhedron* **1998**, *17*, 4535. (d) Collin, J. P.; Jouaiti, A.; Sauvage, J. P. *Inorg. Chem.* **1988**, *27*, 1986−1990. (e) Bernhardt, P. V.; Jones, L. A. *Inorg. Chem.* **1999**, *38*, 5086−5090. (f) Tinnemans, A. H. A.; Koster, T. P. M.; Thewissen, D. H. M. W.; Mackor, A. *Recl. Trav. Chim. Pays-Bas* **1984**, *103*, 288−295. (g) Beley, M.; Collin, J. P.; Ruppert, R.; Sauvage, J. P. *J. Am. Chem. Soc.* **1986**, *108*, 7461−7467.

(7) (a) Chao, T.-H.; Espenson, J. H. *J. Am. Chem. Soc.* **1978**, *100*, 129−133. (b) Du, P.; Knowles, K.; Eisenberg, R. *J. Am. Chem. Soc.* **2008**, *130*, 12576−12577. (c) Du, P.; Schneider, J.; Luo, G.; Brennessel, W. W.; Eisenberg, R. *Inorg. Chem.* **2009**, *48*, 4952−4962. (d) Lazarides, T.; McCormick, T.; Du, P.; Luo, G.; Lindley, B.; Eisenberg, R. *J. Am. Chem. Soc.* **2009**, *131*, 9192−9194. (e) Prokhorova, G. V.; Vinogradova, E. N.; Pronina, N. V. *Zh. Anal. Khim.* **1970**, *25*, 2073−2076. (f) Vinogradova, E. N.; Prokhorova, G. V. *Zh. Anal. Khim.* **1968**, *23*, 1666−1669. (g) Stromberg, A. G.; Zelyanskaya, A. I. *Zh. Obshch. Khim.* **1945**, *15*, 308−318. (h) Lakadamyali, F.; Reisner, E. *Chem. Commun.* **2011**, *47*, 1695−1697.

(8) Adin, A.; Espenson, J. H. *Inorg. Chem.* **1972**, *11*, 686−688.

(9) (a) Paul, N. *J. Electroanal. Chem.* **1967**, *14*, 197−204. (b) Baxter, L. A. M.; Bobrowski, A.; Bond, A. M.; Heath, G. A.; Paul, R. L.; Mrzljak, R.; Zarebski, J. *Anal. Chem.* **1998**, *70*, 1312−1323. (c) Wenrui, J.; Kun, L. *J. Electroanal. Chem.* **1987**, *216*, 181−201.

(10) The thermodynamic potential versus SCE at a given pH under 1 atm H_2 for the electrocatalytic H_2 evolution from water is given by $E(pH) = -0.241$ V $- 0.059$ V(pH).

(11) (a) Malachesky, P. A.; Marcoux, L. S.; Adams, R. N. *J. Phys. Chem.* **1966**, *70*, 4068−4070. (b) Ryan, M. D.; Wei, J.-F.; Feinberg, B. A.; Lau, Y.-K. *Anal. Biochem.* **1979**, *96*, 326−333. (c) Andrieux, C. P.; Dumas-Bouchiat, J. M.; Saveant, J. M. *J. Electroanal. Chem.* **1980**, *113*, 1−18. (d) Wei, J.-F.; Ryan, M. D. *Anal. Biochem.* **1980**, *106*, 269−277. (e) Ng, S. L. L.; Cheh, H. Y. *J. Electrochem. Soc.* **1985**, *132*, 93−98. (f) Machado, R. M.; Chapman, T. W. *J. Electrochem. Soc.* **1987**, *134*, 385−391. (g) Compton, R. G.; Day, M. J.; Laing, M. E.; Northing, R. J.; Penman, J. I.; Waller, A. M. *J. Chem. Soc., Faraday Trans. 1* **1988**, *84*, 2013−2025. (h) Xing, X.; Scherson, D. A. *Anal. Chem.* **1988**, *60*, 1468−1472. (i) Nolan, J. E.; Plambeck, J. A. *J. Electroanal. Chem.* **1990**, *286*, 1−21.

(12) Connolly, P.; Espenson, J. H. *Inorg. Chem.* **1986**, *25*, 2684−2688.

(13) Bakac, A.; Brynildson, M. E.; Espenson, J. H. *Inorg. Chem.* **1986**, *25*, 4108−4114.

(14) Helm, M. L.; Stewart, M. P.; Bullock, R. M.; DuBois, M. R.; DuBois, D. L. *Science* **2011**, *333*, 863−866.

(15) (a) Saveant, J. M.; Vianello, E. *Electrochim. Acta* **1965**, *10*, 905−920. (b) Savéant, J. M.; Vianello, E. *Electrochim. Acta* **1967**, *12*, 629−646. (c) Savéant, J.-M. *Chem. Rev.* **2008**, *108*, 2348−2378.

(16) Sawyer, D. T.; Sobkowiak, A.; Julian, L.; Roberts, J. *Electrochemistry for Chemists*, 2nd ed.; John Wiley & Sons: New York, 1995; pp 86−97.

(17) (a) Anson, F. C. *Acc. Chem. Res.* **1975**, *8*, 400−407. (b) Willett, B. C.; Anson, F. C. *J. Electrochem. Soc.* **1982**, *129*, 1260−1266. (c) Karunadasa, H. I.; Chang, C. J.; Long, J. R. *Nature* **2010**, *464*, 1329−1333.

(18) Schrauzer, G. N. *Inorg. Synth.* **1968**, *11*, 61.

(19) Bakac, A.; Espenson, J. H. *J. Am. Chem. Soc.* **1984**, *106*, 5197−5202.

(20) Costa, G.; Tavagnacco, C.; Puxeddu, A.; Balducci, G.; Kumar, R. *J. Organomet. Chem.* **1987**, *330*, 185−199.

(21) Costa, G.; Mestroni, G.; de Savorgnani, E. *Inorg. Chim. Acta* **1969**, *3*, 323−328.

(22) (a) Jackels, S. C.; Farmery, K.; Barefield, E. K.; Rose, N. J.; Busch, D. H. *Inorg. Chem.* **1972**, *11*, 2893−2901. (b) Tait, A. M.; Busch, D. H. In *Inorganic Syntheses*; Douglas, B. E., Ed.; Wiley Interscience: New York, 1978; Vol. XVIII, pp 22−26.

(23) Long, K. M.; Busch, D. H. *J. Coord. Chem.* **1974**, *4*, 113−123.

(24) Sheldrick, G. *Acta Crystallogr. A* **2008**, *64*, 112−122.

(25) Liaudet, E.; Battaglini, F.; Calvo, E. J. *J. Electroanal. Chem.* **1990**, *293*, 55−68.

(26) Wilhelm, E.; Battino, R.; Wilcock, R. *J. Chem. Rev.* **1977**, *77*, 219−262.